

Total fraction of drug released from diffusion-controlled delivery systems with binding reactions

Elliot J. Carr*

School of Mathematical Sciences, Queensland University of Technology, Brisbane, Australia.

Abstract

In diffusion-controlled drug delivery, it is possible for drug molecules to bind to the carrier material and never be released. A common way to incorporate this phenomenon into the governing mechanistic model is to include an irreversible first-order reaction term, where drug molecules become permanently immobilised once bound. For diffusion-only models, all the drug initially loaded into the device is released, while for reaction-diffusion models only a fraction of the drug is ultimately released. In this short paper, we show how to calculate this fraction for several common diffusion-controlled delivery systems. Easy-to-evaluate analytical expressions for the fraction of drug released are developed for monolithic and core-shell systems of slab, cylinder or sphere geometry. The developed formulas provide analytical insight into the effect that system parameters (e.g. diffusivity, binding rate, core radius) have on the total fraction of drug released, which may be helpful for practitioners designing drug delivery systems.

Keywords: drug delivery, binding, reaction-diffusion, core-shell, release profile.

1 Introduction

Increasingly, mechanistic mathematical models of drug delivery (based on physical conservation laws) are being developed to improve understanding of the transport mechanisms that control the release rate, explore the effect of varying design parameters on the release profile and avoid costly and time consuming experiments [1]. In this field of research, mechanistic mathematical models of *diffusion-controlled* drug delivery are typically based on Fick's second law, where the drug concentration within the system evolves in space and time according to the diffusion equation and specified initial and boundary conditions [2–12]. Such purely-diffusive models yield a release profile $F(t)$ (cumulative amount of drug released over the time interval $[0, t]$ divided by the initial amount of drug loaded into the device) that increases from zero initially to one in the long time limit (Figure 1). Recent experimental work [13], however, has revealed that it is possible for drug to be trapped within the device and never be released due to drug molecules binding to the carrier material [14, 15]. This reduces the amount of drug delivered, resulting in a release profile that approaches a value less than one, denoted in this paper by F_∞ , in the long time limit (Figure 1). Several recent mechanistic models have incorporated binding into the governing diffusion model using an irreversible first-order reaction term, where drug molecules become permanently immobilised once bound [14–17].

In this short paper, we develop a set of analytical expressions for F_∞ for several diffusion-controlled delivery systems with first-order binding reactions. Our study is valid under standard assumptions: the system is radially symmetric (drug concentration is a function of radius and time only), the boundary of the system is stationary (swelling or erosion of the device is negligible) and the drug is initially completely dissolved (drug dissolution is instantaneous). Compact and elegant expressions for F_∞ are provided for both *monolithic* and *core-shell* systems of slab, cylinder or sphere geometry (Figures 2–3). The monolithic system consists of a single homogeneous carrier material (with constant diffusivity) while the core-shell system, consists of two homogeneous “layers” of carrier material (core and shell) with distinct diffusivities. For

*elliott.carr@qut.edu.au

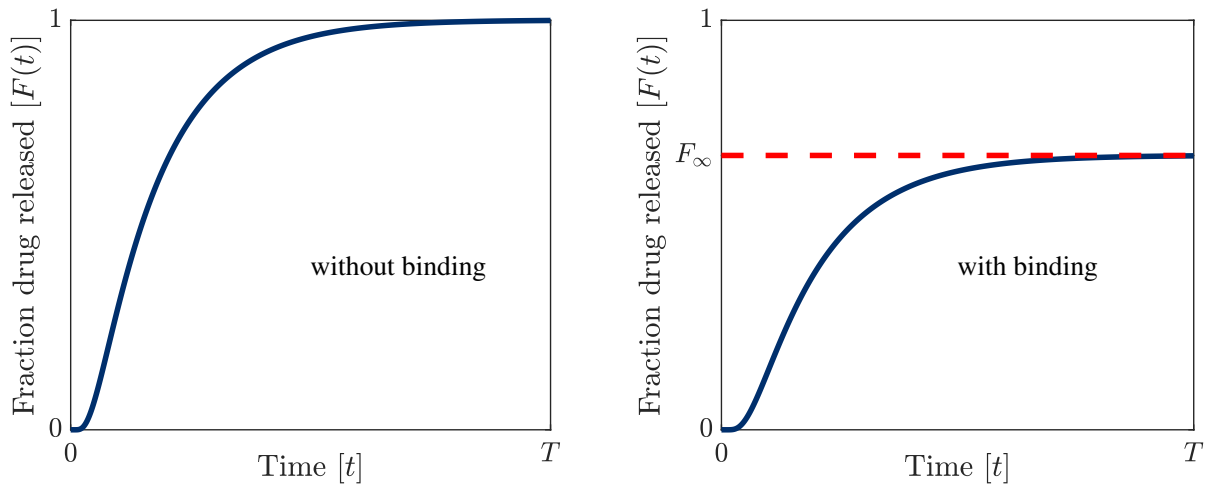


Figure 1: Typical drug release profile, $F(t)$ (cumulative amount of drug released over the time interval $[0, t]$ divided by the initial amount of drug loaded into the device), without binding reactions and with binding reactions. In the long time limit, the fraction of drug released $F_\infty := \lim_{t \rightarrow \infty} F(t) < 1$ with binding.

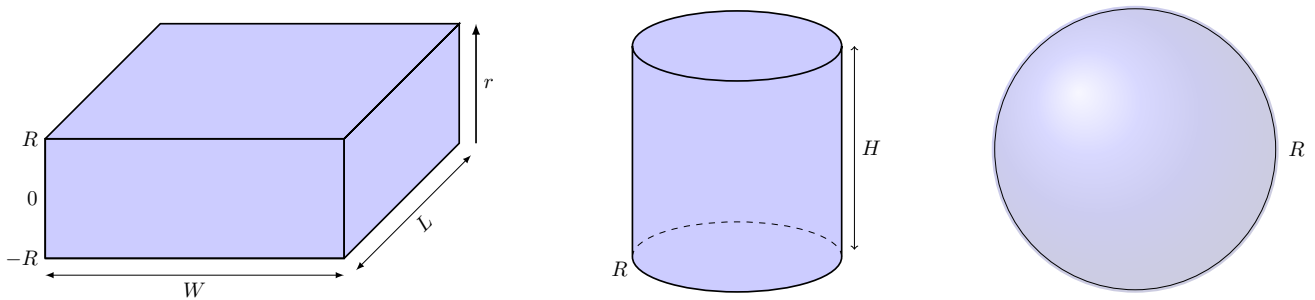


Figure 2: *Monolithic System*. Slab, cylinder and sphere devices of radius R consisting of a single homogeneous carrier material (with constant diffusivity). For the slab, R is assumed to be significantly smaller than both L and W so that drug release is negligible through the minor surfaces (of area $2RL$ or $2RW$) compared to the two major surfaces of the slab (of area LW). For the cylinder, R is significantly smaller than H so that the drug release is negligible through the ends (of area πR^2) compared to the major surface of the cylinder (of area $2\pi RH$). The initial amount of drug is assumed to be homogeneously distributed throughout the device and drug molecules may bind to the carrier material anywhere within the device.

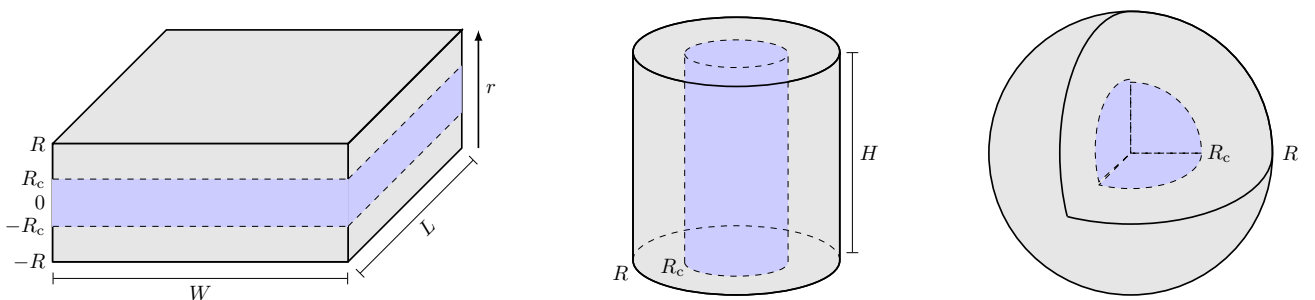


Figure 3: *Core-Shell System*. Slab, cylinder and sphere devices of radius R consisting of two homogeneous “layers” of carrier material (core of radius R_c encapsulated by a shell) with distinct diffusivities. For the slab, R is assumed to be significantly smaller than both L and W so that drug release is negligible through the minor surfaces (of area $2RL$ or $2RW$) compared to the two major surfaces of the slab (of area LW). For the cylinder, R is significantly smaller than H so that the drug release is negligible through the ends (of area πR^2) compared to the major surface of the cylinder (of area $2\pi RH$). The initial amount of drug is assumed to be homogeneously distributed throughout the core only and drug molecules may bind to the carrier material within the shell only.

the monolithic system, the initial amount of drug is assumed to be homogeneously distributed throughout the system while for the core-shell system, the initial amount of drug is assumed to be homogeneously distributed throughout the core only. For the monolithic system, drug molecules may bind to the carrier material anywhere within the device while for the core-shell system, drug molecules may bind to the carrier material within the shell only [15]. Both the monolithic and core-shell systems are encapsulated in a thin coating (shell) that is either fully-permeable (no resistance to drug release) or semi-permeable (finite resistance to drug released) [8]. In total, 12 distinct expressions for F_∞ are derived, one for each combination of system type (monolithic, core-shell), device geometry (slab, cylinder, sphere) and coating permeability (fully-permeable, semi-permeable). Each expression explains how the value of F_∞ changes for general values of the model parameters (e.g. diffusivity, reaction rate, surface transfer coefficient).

The remaining sections of this paper discuss how the expressions for F_∞ are developed for the monolithic and core-shell systems, respectively. Analytical and numerical evidence is then presented supporting the derived results.

2 Monolithic System

For the monolithic system, the drug dynamics are assumed to be governed by the reaction-diffusion model:

$$\frac{\partial c}{\partial t} = \frac{D}{r^{d-1}} \frac{\partial}{\partial r} \left(r^{d-1} \frac{\partial c}{\partial r} \right) - kc, \quad 0 < r < R, \quad (1)$$

$$c(r, 0) = c_0, \quad (2)$$

$$\begin{cases} \frac{\partial c}{\partial r}(0, t) = 0, & \text{if } d = 1, \\ c(0, t) \text{ finite,} & \text{if } d = 2, 3, \end{cases} \quad \begin{cases} c(R, t) = 0, & \text{if fully-permeable,} \\ -D \frac{\partial c}{\partial r}(R, t) = Pc(R, t), & \text{if semi-permeable,} \end{cases} \quad (3)$$

where d specifies the geometry ($d = 1, 2, 3$ for the slab, cylinder and sphere, respectively), $c(r, t)$ is the drug concentration, R is the device radius (Figure 2), D is the diffusivity, k is the binding rate, c_0 is the initial uniform drug concentration and P is the surface transfer coefficient. Note that the surface boundary condition (at $r = R$) depends on whether the coating is fully-permeable or semi-permeable with equivalence obtained in the limit as the surface transfer coefficient P tends to infinity. Mathematically, the total fraction of drug released F_∞ is given by the integral of the concentration flux over the release surface(s) divided by the initial amount of drug loaded into the device, which as shown in Appendix A.1 simplifies to

$$F_\infty = \frac{d}{Rc_0} \int_0^\infty -D \frac{\partial c}{\partial r}(R, t) dt, \quad (4)$$

under radial symmetry. In Appendix A.2, we show further that F_∞ can be expressed as

$$F_\infty = 1 - \frac{kd}{R^d c_0} \int_0^R r^{d-1} \mathcal{C}(r) dr, \quad (5)$$

where $\mathcal{C}(r)$ satisfies the boundary value problem:

$$\frac{D}{r^{d-1}} \frac{d}{dr} \left(r^{d-1} \frac{d\mathcal{C}}{dr} \right) - k\mathcal{C} = -c_0, \quad (6)$$

$$\begin{cases} \frac{\partial c}{\partial r}(0, t) = 0, & \text{if } d = 1, \\ c(0, t) \text{ finite,} & \text{if } d = 2, 3, \end{cases} \quad \begin{cases} c(R, t) = 0, & \text{if fully-permeable,} \\ -D \frac{\partial c}{\partial r}(R, t) = Pc(R, t), & \text{if semi-permeable.} \end{cases} \quad (7)$$

The attraction here is that the above boundary value problem admits exact analytical solutions involving hyperbolic ($d = 1, 3$) and Bessel functions ($d = 2$) that can be found by hand or using a computer algebra system. Solving the boundary value problem (6)–(7) separately for $d = 1, 2, 3$, and evaluating the integral in (5) yields the expressions for F_∞ given below in equations (8)–(13). For $d = 2$, the expressions for F_∞ involve I_0 and I_1 , the modified Bessel functions of the first kind of zero and first order respectively.

Fully-permeable coating

$$\text{Slab} \quad F_\infty = \frac{\sinh(\lambda)}{\lambda \cosh(\lambda)} \quad (8)$$

$$\text{Cylinder} \quad F_\infty = \frac{2I_1(\lambda)}{\lambda I_0(\lambda)} \quad (9)$$

$$\text{Sphere} \quad F_\infty = \frac{3[\lambda \cosh(\lambda) - \sinh(\lambda)]}{\lambda^2 \sinh(\lambda)} \quad (10)$$

where $\lambda = \sqrt{\frac{kR^2}{D}}$.

Semi-permeable coating

$$\text{Slab} \quad F_\infty = \frac{\mathcal{P} \sinh(\lambda)}{\lambda[\lambda \sinh(\lambda) + \mathcal{P} \cosh(\lambda)]} \quad (11)$$

$$\text{Cylinder} \quad F_\infty = \frac{2\mathcal{P}I_1(\lambda)}{\lambda[\lambda I_1(\lambda) + \mathcal{P}I_0(\lambda)]} \quad (12)$$

$$\text{Sphere} \quad F_\infty = \frac{3\mathcal{P}[\lambda \cosh(\lambda) - \sinh(\lambda)]}{\lambda^2[\lambda \cosh(\lambda) + (\mathcal{P} - 1) \sinh(\lambda)]} \quad (13)$$

where $\lambda = \sqrt{\frac{kR^2}{D}}$ and $\mathcal{P} = \frac{PR}{D}$.

The above results reveal how F_∞ depends on a single dimensionless variable (λ) for the fully-permeable coating and two dimensionless variables (λ , \mathcal{P}) for the semi-permeable coating. Studying these expressions, we see that equivalence between the semi-permeable and permeable cases is obtained when $P \rightarrow \infty$. This fact together with the observation that the terms independent of P in the denominators of equations (11)–(13) are positive, means that F_∞ is always smaller for the semi-permeable case than the corresponding fully-permeable case. This observation can be explained by the surface resistance resulting in drug molecules remaining in the device longer, increasing the likelihood that they bind to the carrier material and never be released. In summary, the above expressions provide the total fraction of drug released from the monolithic device (total amount of drug released divided by the initial amount of drug loaded into the device) for general values of the diffusivity (D), binding rate (k), device radius (R) and surface transfer coefficient (P). Similar expressions to those above appear in the classical text [18] for the dual process of absorption into a cylinder/sphere from the surrounding medium.

Finally, we note that the actual amount of drug released is obtained by multiplying F_∞ by the initial amount of drug loaded into the device:

$$\begin{cases} 2Rc_0LW, & \text{if } d = 1, \\ \pi R^2c_0H, & \text{if } d = 2, \\ 4\pi R^3c_0/3, & \text{if } d = 3, \end{cases}$$

where L , W and H are defined in Figure 2.

3 Core-Shell System

For the core-shell system, the drug dynamics are assumed to be governed by the reaction-diffusion model:

$$\frac{\partial c_c}{\partial t} = \frac{D_c}{r^{d-1}} \frac{\partial}{\partial r} \left(r^{d-1} \frac{\partial c_c}{\partial r} \right), \quad 0 < r < R_c, \quad (14)$$

$$\frac{\partial c_s}{\partial t} = \frac{D_s}{r^{d-1}} \frac{\partial}{\partial r} \left(r^{d-1} \frac{\partial c_s}{\partial r} \right) - k_s c_s, \quad R_c < r < R, \quad (15)$$

$$c_c(r, 0) = c_0, \quad c_s(r, 0) = 0, \quad (16)$$

$$c_c(R_c, t) = c_s(R_c, t), \quad D_c \frac{\partial c_c}{\partial r}(R_c, t) = D_s \frac{\partial c_s}{\partial r}(R_c, t), \quad (17)$$

$$\begin{cases} \frac{\partial c_c}{\partial r}(0, t) = 0, & \text{if } d = 1, \\ c_c(0, t) \text{ finite,} & \text{if } d = 2, 3, \end{cases} \quad \begin{cases} c_s(R, t) = 0, & \text{if fully-permeable,} \\ -D_s \frac{\partial c_s}{\partial r}(R, t) = P c_s(R, t), & \text{if semi-permeable,} \end{cases} \quad (18)$$

where d specifies the geometry ($d = 1, 2, 3$ for the slab, cylinder and sphere, respectively), $c_c(r, t)$ is the drug concentration in the core ($0 < r < R_c$), $c_s(r, t)$ is the drug concentration in the shell ($R_c < r < R$), D_c is the diffusivity in the core, D_s is the diffusivity in the shell, k_s is the binding rate (shell only), c_0 is the initial uniform drug concentration (core only) and P is the surface transfer coefficient. For the core-shell system, the total fraction of drug released is given by (see Appendix A.3):

$$F_\infty = \frac{dR^{d-1}}{R_c^d c_0} \int_0^\infty -D_s \frac{\partial c_s}{\partial r}(R, t) dt. \quad (19)$$

In Appendix A.4, we show that F_∞ can be expressed as:

$$F_\infty = 1 - \frac{k_s d}{R_c^d c_0} \int_{R_c}^R r^{d-1} \mathcal{C}_s(r) dr, \quad (20)$$

where $\mathcal{C}_s(r)$ satisfies the following boundary value problem:

$$\frac{D_c}{r^{d-1}} \frac{d}{dr} \left(r^{d-1} \frac{d\mathcal{C}_c}{dr} \right) = -c_0, \quad 0 < r < R_c, \quad (21)$$

$$\frac{D_s}{r^{d-1}} \frac{d}{dr} \left(r^{d-1} \frac{d\mathcal{C}_s}{dr} \right) - k_s \mathcal{C}_s = 0, \quad R_c < r < R, \quad (22)$$

$$\mathcal{C}_c(R_c) = \mathcal{C}_s(R_c), \quad D_c \frac{d\mathcal{C}_c}{dr}(R_c) = D_s \frac{d\mathcal{C}_s}{dr}(R_c), \quad (23)$$

$$\begin{cases} \frac{d\mathcal{C}_c}{dr}(0) = 0, & \text{if } d = 1, \\ \mathcal{C}_c(0) \text{ finite,} & \text{if } d = 2, 3, \end{cases} \quad \begin{cases} \mathcal{C}_s(R) = 0, & \text{if fully-permeable,} \\ -D_s \frac{d\mathcal{C}_s}{dr}(R) = P \mathcal{C}_s(R), & \text{if semi-permeable.} \end{cases} \quad (24)$$

As for the monolithic system, the above boundary value problem admits exact analytical solutions involving hyperbolic ($d = 1, 3$) and Bessel functions ($d = 2$) that can be found by hand (quite tediously) or using a computer algebra system. Solving the boundary value problem (21)–(24) separately for $d = 1, 2, 3$ and evaluating the integral in (20) yields the expressions for F_∞ given below in equations (25)–(30). For $d = 2$, the expressions for F_∞ involve I_0 and I_1 , the modified Bessel functions of the first kind of zero and first order respectively and K_0 and K_1 , the modified Bessel functions of the second kind of zero and first order respectively.

Fully-permeable coating

$$\textit{Slab} \quad F_\infty = \frac{1}{\cosh(\lambda_s \mathcal{R}_s)} \quad (25)$$

$$\textit{Cylinder} \quad F_\infty = \frac{1}{\mathcal{R}_c \lambda_s [K_0(\lambda_s) I_1(\mathcal{R}_c \lambda_s) + I_0(\lambda_s) K_1(\mathcal{R}_c \lambda_s)]} \quad (26)$$

$$\textit{Sphere} \quad F_\infty = \frac{\lambda_s}{\sinh(\lambda_s \mathcal{R}_s) + \lambda_s \mathcal{R}_c \cosh(\lambda_s \mathcal{R}_s)} \quad (27)$$

where $\lambda_s = \sqrt{\frac{k_s R^2}{D_s}}$, and $\mathcal{R}_c = \frac{R_c}{R}$.

Semi-permeable coating

$$\text{Slab} \quad F_\infty = \frac{\mathcal{P}_s}{\mathcal{P}_s \cosh(\lambda_s \mathcal{R}_s) + \lambda_s \sinh(\lambda_s \mathcal{R}_s)} \quad (28)$$

$$\text{Cylinder} \quad F_\infty = \frac{\mathcal{P}_s}{\mathcal{R}_c \lambda_s ([\mathcal{P}_s K_0(\lambda_s) - \lambda_s K_1(\lambda_s)] I_1(\mathcal{R}_c \lambda_s) + [\mathcal{P}_s I_0(\lambda_s) + \lambda_s I_1(\lambda_s)] K_1(\mathcal{R}_c \lambda_s))} \quad (29)$$

$$\text{Sphere} \quad F_\infty = \frac{\mathcal{P}_s \lambda_s}{(\mathcal{P}_s - 1 + \mathcal{R}_c \lambda_s^2) \sinh(\lambda_s \mathcal{R}_s) + \lambda_s (\mathcal{R}_s + \mathcal{P}_s \mathcal{R}_c) \cosh(\lambda_s \mathcal{R}_s)} \quad (30)$$

where $\lambda_s = \sqrt{\frac{k_s R^2}{D_s}}$, $\mathcal{P}_s = \frac{PR}{D_s}$, $\mathcal{R}_c = \frac{R_c}{R}$ and $\mathcal{R}_s = 1 - \mathcal{R}_c$.

The above results reveal how F_∞ depends on two dimensionless variables (λ_s , \mathcal{R}_c) for the fully-permeable coating and three dimensionless variables (λ_s , \mathcal{R}_c and \mathcal{P}_s) for the semi-permeable coating. Interestingly (perhaps unexpectedly), F_∞ is independent of the diffusivity in the core D_c in all cases. As for the monolithic system, F_∞ is always smaller for the semi-permeable case with equivalence obtained when $P \rightarrow \infty$. In summary, the above expressions provide the total fraction of drug released from the core-shell device (total amount of drug released divided by the initial amount of drug loaded into the device) for general values of the core diffusivity (D_c), shell diffusivity (D_s), shell binding rate (k_s), core radius (R_c), device radius (R) and surface transfer coefficient (P).

Finally, we note that the actual amount of drug released is obtained by multiplying F_∞ by the initial amount of drug loaded into the device:

$$\begin{cases} 2R_c c_0 LW, & \text{if } d = 1, \\ \pi R_c^2 c_0 H, & \text{if } d = 2, \\ 4\pi R_c^3 c_0 / 3, & \text{if } d = 3, \end{cases}$$

where L , W and H are defined in Figure 3.

4 Supporting Numerical Experiments

The analytical expressions for F_∞ derived in the previous sections have been verified analytically using MATLAB's symbolic toolbox. Results in Figures 4 and 5 also provide evidence to support the derived expressions for a set of parameter values [16]. These figures compare computed values of F_∞ to the long time limiting behaviour of the cumulative fraction of drug released:

$$F(t) = \begin{cases} \frac{d}{Rc_0} \int_0^t -D \frac{\partial c}{\partial r}(R, \tau) d\tau, & \text{if monolithic system,} \\ \frac{dR^{d-1}}{R_c^d c_0} \int_0^t -D_s \frac{\partial c_s}{\partial r}(R, \tau) d\tau, & \text{if core-shell system.} \end{cases} \quad (31)$$

To compute $F(t)$ we solve the governing reaction-diffusion model, equations (1)–(3) for the monolithic system and (14)–(18) for the core-shell system, numerically by (i) discretising over space $[0, R]$ using a finite volume method with N_r uniformly spaced nodes and (ii) discretising over time $[0, T]$ using the backward Euler method with N_t time steps of fixed duration. Here T is chosen to be sufficiently large to capture the long time limiting behaviour of $F(t)$. The numerical method computes discrete approximations to the concentration $c(r_k, t_i)$ for $k = 1, \dots, N_r$ and $i = 1, \dots, N_t$, where $r_k = (k - 1)R / (N_r - 1)$ and $t_i = iT / N_t$. The numerical approximations to $c(r_k, t_i)$ for $k = 1, \dots, N_r$ are then used to compute $F(t_i)$ for $i = 1, \dots, N_t$ by applying a backward difference approximation to the radial concentration gradient in (31) followed by a trapezoidal rule approximation to the integral over $[0, t_i]$ in (31). Comparisons in Figures 4 and 5 are given for $N_r = 2001$ spatial nodes and $N_t = 10^4$ time steps with excellent agreement reported between the computed values of F_∞ and $F(T)$ across all combination of system type (monolithic, core-shell), device geometry (slab, cylinder, sphere) and coating permeability (fully-permeable, semi-permeable). Full details on both the analytical and numerical verification are available in our MATLAB code, which is available on GitHub at <https://github.com/elliottcarr/Carr2024a>.

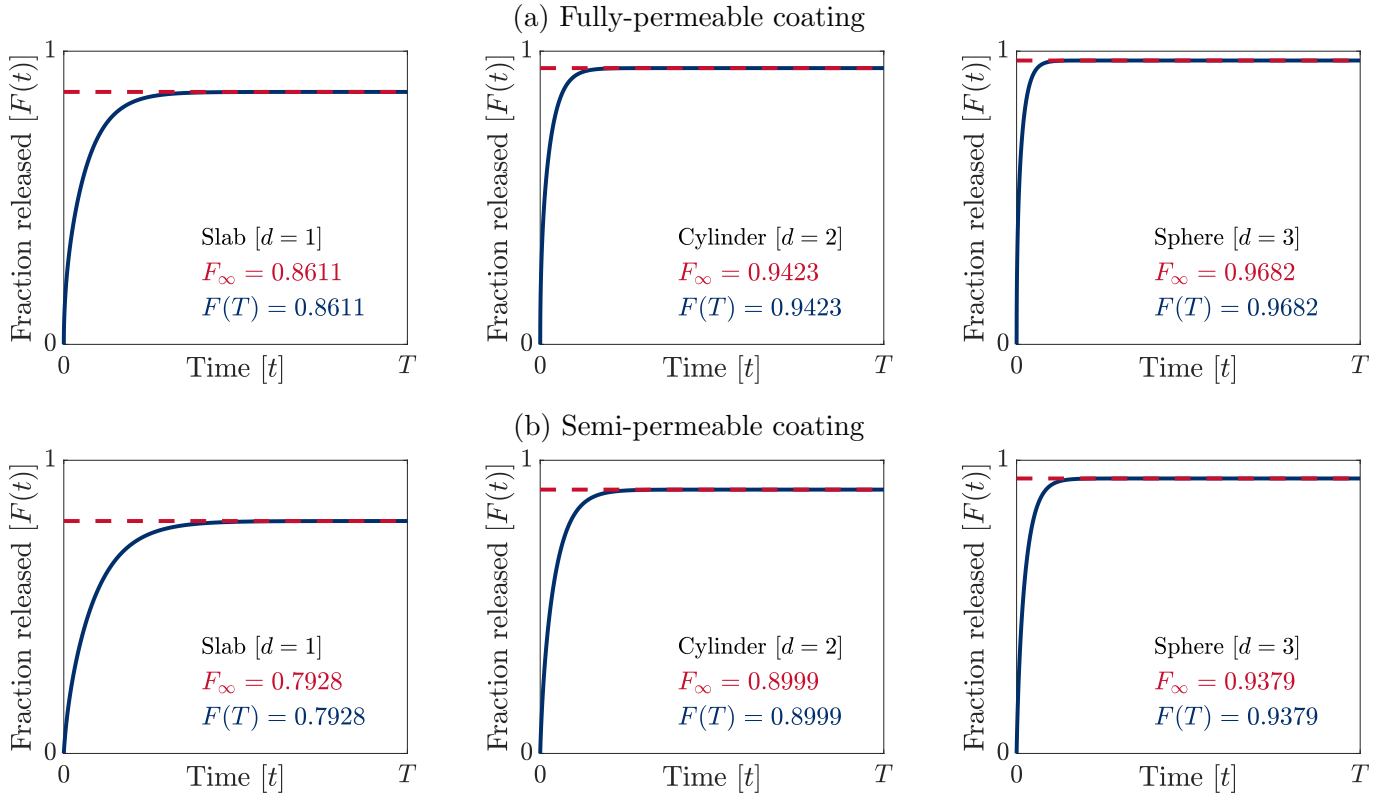


Figure 4: *Monolithic System*. Comparing the analytical expressions for F_∞ (8)–(13) to numerical approximations of $F(T)$, where T is sufficiently large to capture the long time limiting behaviour of $F(t)$. Parameter values: $c_0 = 0.4 \text{ mol cm}^{-3}$, $R = 10^{-4} \text{ cm}$, $D = 10^{-12} \text{ cm}^2 \text{ s}^{-1}$, $k = 5 \times 10^{-5} \text{ s}^{-1}$, $T = 5 \times 10^4 \text{ s}$ (dimensional), $\lambda = \sqrt{0.5}$, $\mathcal{P} = 5$ (dimensionless).

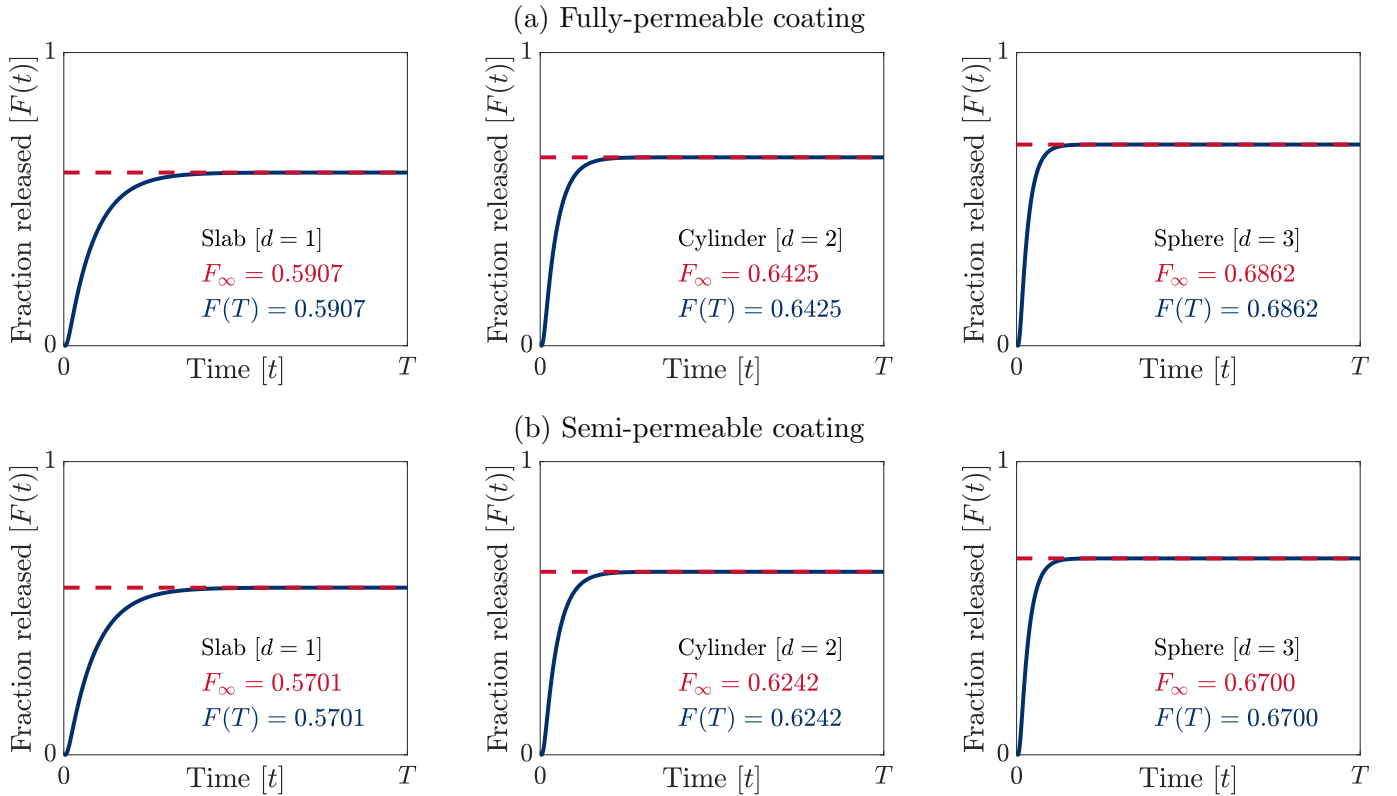


Figure 5: *Core-Shell System*. Comparing the analytical expressions for F_∞ (25)–(30) to numerical approximations of $F(T)$, where T is sufficiently large to capture the long time limiting behaviour of $F(t)$. Parameter values: $c_0 = 0.4 \text{ mol cm}^{-3}$, $R_c = 0.5 \times 10^{-4} \text{ cm}$, $R = 10^{-4} \text{ cm}$, $D_c = 10^{-11} \text{ cm}^2 \text{ s}^{-1}$, $D_s = 10^{-13} \text{ cm}^2 \text{ s}^{-1}$, $k_s = 5 \times 10^{-5} \text{ s}^{-1}$, $T = 3 \times 10^5 \text{ s}$ (dimensional), $\lambda_s = \sqrt{5}$, $\mathcal{P}_s = 50$, $\mathcal{R}_c = 0.5$ (dimensionless).

5 Conclusions

In summary, we have developed a set of analytical expressions to calculate F_∞ (total amount of drug released divided by the initial amount of drug) for several diffusion-controlled delivery systems in the presence of binding reactions. In total, 12 distinct expressions for F_∞ were derived, one for each combination of system type (monolithic, core-shell), device geometry (slab, cylinder, sphere) and coating permeability (fully-permeable, semi-permeable). Each expression provides analytical insight into the effect that particular physical and geometrical parameters (device geometry, diffusivity, binding rate, surface transfer coefficient) have on the value of F_∞ ; insight which may be helpful for practitioners designing drug delivery systems.

While we have considered a wide-range of delivery systems in this work, it is important to note that the results are limited to the specific device configurations presented. Extending the analysis for the core-shell system to explore, for example, binding reactions in the core and/or non-zero initial drug concentration in the shell would yield different expressions for F_∞ .

A Appendices

A.1 Monolithic System: Initial form for F_∞

The total fraction of drug released, defined as the integral of the concentration flux through the release surface(s) (ω) scaled by the initial amount of drug loaded into the device region (Ω), simplifies to (4) as follows

$$F_\infty = \frac{\int_0^\infty \iint_\omega [-D\nabla c \cdot \mathbf{n} dA] dt}{\iint_\Omega c_0 dV} = \frac{|\omega| \int_0^\infty -D \frac{\partial c}{\partial r}(R, t) dt}{|\Omega| c_0} = \frac{d}{R c_0} \int_0^\infty -D \frac{\partial c}{\partial r}(R, t) dt,$$

due to radial symmetry and the fact that $|\omega|/|\Omega|$ equals the surface area of the $(d-1)$ -dimensional sphere of radius R divided by the volume of the d -dimensional ball of radius R (LW and H cancel from both the numerator and denominator for the slab and cylinder, respectively).

A.2 Monolithic System: Alternative form for F_∞

In this appendix, we demonstrate equivalence of the two forms of F_∞ given in equations (4) and (5). Integrating the reaction-diffusion equation (1) over the slab, cylinder and sphere yields

$$\int_0^R r^{d-1} \frac{\partial c}{\partial t} dr = D \int_0^R \frac{\partial}{\partial r} \left(r^{d-1} \frac{\partial c}{\partial r} \right) dr - k \int_0^R r^{d-1} c dr,$$

due to radial symmetry. Reversing the order of integration and differentiation on the left and evaluating the first integral on the right produces:

$$\frac{d}{dt} \left[\int_0^R r^{d-1} c dr \right] = R^{d-1} \left[D \frac{\partial c}{\partial r}(R, t) \right] - k \int_0^R r^{d-1} c dr,$$

and hence:

$$R^{d-1} \left[-D \frac{\partial c}{\partial r}(R, t) \right] = -\frac{d}{dt} \left[\int_0^R r^{d-1} c dr \right] - k \int_0^R r^{d-1} c dr.$$

Integrating this last equation over the time interval $[0, \infty)$, using the initial condition (2) and the fact that $c(r, t)$ tends to zero at infinite time yields:

$$R^{d-1} \int_0^\infty \left[-D \frac{\partial c}{\partial r}(R, t) \right] dt = \int_0^R r^{d-1} c_0 dr - k \int_0^R r^{d-1} \mathcal{C}(r) dr,$$

where $\mathcal{C}(r) := \int_0^\infty c(r, t) dt$. Dividing both sides of this last equation by $\int_0^R r^{d-1} c_0 dr = R^d c_0 / d$ then gives the desired result:

$$\frac{d}{R c_0} \int_0^\infty -D \frac{\partial c}{\partial r}(R, t) dt = 1 - \frac{k d}{R^d c_0} \int_0^R r^{d-1} \mathcal{C}(r) dr.$$

To complete the demonstration, we need to show that $\mathcal{C}(r)$ satisfies the boundary value problem (6)–(7). The differential equation (6) is obtained by integrating the reaction-diffusion equation (1) over the time interval $[0, \infty)$, using the initial condition (2) and the fact that $c(r, t)$ tends to zero at infinite time:

$$-c_0 = \int_0^\infty \frac{D}{r^{d-1}} \frac{\partial}{\partial r} \left(r^{d-1} \frac{\partial c}{\partial r} \right) dt - k \int_0^\infty c(r, t) dt,$$

which simplifies to equation (6) when reversing the order of differentiation and integration in the second term on the right and introducing $C(r) := \int_0^\infty c(r, t) dt$. Finally, the boundary conditions (7) are obtained by integrating the boundary conditions (3) over the time interval $[0, \infty)$:

$$\begin{cases} \int_0^\infty \frac{\partial c}{\partial r}(0, t) dt = 0, & \text{if } d = 1, \\ \int_0^\infty c(0, t) dt \text{ finite,} & \text{if } d = 2, 3, \end{cases} \quad \begin{cases} \int_0^\infty c(R, t) dt = 0, & \text{if fully-permeable,} \\ -D \int_0^\infty \frac{\partial c}{\partial r}(R, t) dt = P \int_0^\infty c(R, t) dt, & \text{if semi-permeable,} \end{cases}$$

and reversing the order of differentiation and integration as appropriate.

A.3 Core-Shell System: Initial form for F_∞

The total fraction of drug released, defined as the integral of the concentration flux through the release surface(s) (ω) scaled by the initial amount of drug loaded into the core region (Ω_c), simplifies to (19) as follows:

$$F_\infty = \frac{\int_0^\infty [\int_\omega -D_s \nabla c_s \cdot \mathbf{n} dA] dt}{\int_{\Omega_c} c_0 dV} = \frac{|\omega| \int_0^\infty -D \frac{\partial c}{\partial r}(R, t) dt}{|\Omega_c| c_0} = \frac{dR^{d-1}}{R_c^d c_0} \int_0^\infty -D_s \frac{\partial c_s}{\partial r}(R, t) dt,$$

due to radial symmetry and the fact that $|\omega|/|\Omega_c|$ equals the surface area of the $(d-1)$ -dimensional sphere of radius R divided by the volume of the d -dimensional ball of radius R_c (LW and H cancel from both the numerator and denominator for the slab and cylinder, respectively).

A.4 Core-Shell System: Alternative form for F_∞

In this appendix, we demonstrate equivalence of the two forms of F_∞ given in equations (19) and (20). Integrating the reaction-diffusion equation (14)–(15) over the slab, cylinder and sphere yields

$$\int_0^{R_c} r^{d-1} \frac{\partial c_c}{\partial t} dr + \int_{R_c}^R r^{d-1} \frac{\partial c_s}{\partial t} dr = D_c \int_0^{R_c} \frac{\partial}{\partial r} \left(r^{d-1} \frac{\partial c_c}{\partial r} \right) dr + D_s \int_{R_c}^R \frac{\partial}{\partial r} \left(r^{d-1} \frac{\partial c_s}{\partial r} \right) dr - k_s \int_{R_c}^R r^{d-1} c_s dr,$$

due to radial symmetry. Reversing the order of integration and differentiation on the left, evaluating the first two integrals on the right and using the second interface condition (17) yields:

$$\frac{d}{dt} \left[\int_0^{R_c} r^{d-1} c_c dr + \int_{R_c}^R r^{d-1} c_s dr \right] = R^{d-1} \left[D_s \frac{\partial c_s}{\partial r}(R, t) \right] - k_s \int_{R_c}^R r^{d-1} c_s dr,$$

and hence:

$$R^{d-1} \left[-D_s \frac{\partial c_s}{\partial r}(R, t) \right] = -\frac{d}{dt} \left[\int_0^{R_c} r^{d-1} c_c dr + \int_{R_c}^R r^{d-1} c_s dr \right] - k_s \int_{R_c}^R r^{d-1} c_s dr.$$

Integrating this last equation over the time interval $[0, \infty)$, using the initial condition (16) and the fact that both $c_c(r, t)$ and $c_s(r, t)$ tend to zero at infinite time yields:

$$R^{d-1} \int_0^\infty \left[-D_s \frac{\partial c_s}{\partial r}(R, t) \right] dt = \int_0^{R_c} r^{d-1} c_0 dr - k_s \int_{R_c}^R r^{d-1} \mathcal{C}_s(r) dr,$$

where we have set $\mathcal{C}_s(r) := \int_0^\infty c_s(r, t) dt$. Dividing both sides of this last equation by $\int_0^{R_c} r^{d-1} c_0 dr = (R_c^d c_0)/d$ yields the desired result:

$$\frac{dR^{d-1}}{c_0 R_c^d} \int_0^\infty -D_s \frac{\partial c_s}{\partial r}(R, t) dt = 1 - \frac{k_s d}{R_c^d c_0} \int_{R_c}^R r^{d-1} \mathcal{C}_s(r) dr.$$

To complete the demonstration, we need to show that $C_s(r)$ satisfies the boundary value problem (21)–(24). The differential equations (21)–(22) are obtained by integrating the reaction-diffusion equations (14)–(15) over the time interval $[0, \infty)$, using the initial condition (16) and the fact that both $c_c(r, t)$ and $c_s(r, t)$ tend to zero at infinite time:

$$\begin{aligned} -c_0 &= \int_0^\infty \frac{D}{r^{d-1}} \frac{\partial}{\partial r} \left(r^{d-1} \frac{\partial c_c}{\partial r} \right) dt, & 0 < r < R_c, \\ 0 &= \int_0^\infty \frac{D}{r^{d-1}} \frac{\partial}{\partial r} \left(r^{d-1} \frac{\partial c_s}{\partial r} \right) dt - k_s \int_0^\infty c_s(r, t) dt, & R_c < r < R, \end{aligned}$$

which simplify to equations (21)–(22) when reversing the order of differentiation and integration in the second term on the right of both equations and introducing $C_c(r) := \int_0^\infty c_c(r, t) dt$ and $C_s(r) := \int_0^\infty c_s(r, t) dt$. Finally, the interface and boundary conditions (23)–(24) are obtained by integrating the interface and boundary conditions (17)–(18) over the time interval $[0, \infty)$ [19]:

$$\begin{cases} \int_0^\infty \frac{\partial c_c}{\partial r}(0, t) dt = 0, & \text{if } d = 1, \\ \int_0^\infty c_c(0, t) dt \text{ finite,} & \text{if } d = 2, 3, \end{cases} \quad \begin{cases} \int_0^\infty c_s(R, t) dt = 0, & \text{if fully-permeable,} \\ -D \int_0^\infty \frac{\partial c_s}{\partial r}(R, t) dt = P \int_0^\infty c_s(R, t) dt, & \text{if semi-permeable,} \end{cases}$$

and reversing the order of differentiation and integration as appropriate.

References

- [1] J. Siepmann and F. Siepmann, Modeling of diffusion controlled drug delivery, *Journal of Controlled Release*, 161 (2012) 351–362.
- [2] D. Y. Arifin, L. Y. Lee and C-H Wang, Mathematical modeling and simulation of drug release from microspheres: Implications to drug delivery systems, *Advanced Drug Delivery Reviews* 58 (2006) 1274–1325.
- [3] E. J. Carr and G. Pontrelli, Modelling mass diffusion for a multi-layer sphere immersed in a semi-infinite medium: application to drug delivery, *Mathematical Biosciences* 303 (2018) 1–9.
- [4] E. J. Carr, Exponential and Weibull models for spherical and spherical-shell diffusion-controlled release systems with semi-absorbing boundaries, *Physica A* 605 (2022) 127985.
- [5] M. S. Gomes-Filho, M. A. A. Barbosa, F. A. Oliveira, A statistical mechanical model for drug release: Relations between release parameters and porosity, *Physica A* 540 (2020) 123165.
- [6] A. Hadjithodorou and G. Kalosakas, Analytical and numerical study of diffusion-controlled drug release from composite spherical matrices, *Materials Science and Engineering C* 42 (2014) 681–690.
- [7] M. Ignacio and G. W. Slater, Using fitting functions to estimate the diffusion coefficient of drug molecules in diffusion-controlled release systems, *Physica A* 567 (2021) 125681.
- [8] B. Kaoui, M. Lauricella, G. Pontrelli, Mechanistic modelling of drug release from multi-layer capsules, *Computers in Biology and Medicine*, 93 (2018) 149–157.
- [9] N. A. Peppas and B. Narasimhand, Mathematical models in drug delivery: How modeling has shaped the way we design new drug delivery systems, *Journal of Controlled Release* 190 (2014) 75–81.
- [10] P. L. Ritger and N. A. Peppas, A simple equation for description of solute release. I. Fickian and non-Fickian release from non-swellable devices in the form of slabs, spheres, cylinders or discs, *Journal of Controlled Release* 5 (1987) 23–36.
- [11] J. Siepmann and F. Siepmann, Mathematical modeling of drug delivery, *International Journal of Pharmaceutics*, 364 (2008) 328–343.
- [12] L. Simon and J. Ospina, Controlled drug release from a spheroidal matrix, *Physica A* 518 (2019) 30–37.
- [13] G. Toniolo, M. Louka, G. Menounou, N. Z. Fantoni, G. Mitrikas, E. K. Efthimiadou, A. Masi, M. Bortolotti, L. Polito, A. Bolognesi, A. Kellett, C. Ferreri, C. Chatgililoglu, [Cu(TPMA)(Phen)](ClO₄)₂: Metallo-drug Nanocontainer Delivery and Membrane Lipidomics of a Neuroblastoma Cell Line Coupled with a Liposome Biomimetic Model Focusing on Fatty Acid Reactivity, *ACS Omega* 3 (2018) 15952–15965
- [14] A. Jain, S. McGinty, G. Pontrelli, L. Zhou, Theoretical model for diffusion-reaction based drug delivery from a multilayer spherical capsule, *International Journal of Heat and Mass Transfer*, 183 (2022) 122072.
- [15] G. Pontrelli, G. Toniolo, S. McGinty, D. Peri, S. Succi, C. Chatgililoglu, Mathematical modelling of drug delivery from pH-responsive nanocontainers, *Computers in Biology and Medicine*, 131 (2021) 104238.
- [16] E. J. Carr, G. Pontrelli, Modelling functionalized drug release for a spherical capsule, *International Journal of Heat and Mass Transfer* 222 (2024) 125065.
- [17] S. McGinty and G. Pontrelli, A general model of coupled drug release and tissue absorption for drug delivery devices, *Journal of Controlled Release* 217 (2015) 327–336.
- [18] J. Crank, *The Mathematics of Diffusion*, Oxford University Press, 1975.
- [19] E. J. Carr and C. J. Wood, Rear-surface integral method for calculating thermal diffusivity: Finite pulse time correction and two-layer samples, *International Journal of Heat and Mass Transfer* 144 (2019) 118609.